

The dimensional stability of glass-fibre reinforced Polyamide 66 during hydrolysis conditioning.

J. L. Thomason and J.Z.Ali

University of Strathclyde, Department of Mechanical Engineering, 75 Montrose Street, Glasgow G1 1XJ, United Kingdom.

Abstract

Injection moulded glass-fibre reinforced polyamide 66 composites based on two glass fibre products with different sizing formulations and unreinforced polymer samples have been characterised both dry as moulded and during conditioning in a water-glycol mixture at 70°C for a range of times up to 400 hours. The results reveal that hydrothermal ageing in water-glycol mixtures causes significant changes in the weight and dimensions of these materials. All conditioned materials showed a time dependent weight increase which could be characterised as pseudo-Fickian. The weight change could be well modelled by a Fickian diffusion process with a time dependent diffusion coefficient. It was not apparent that changing the glass fibre sizing affected the dimensional stability of the composites. There was a strong correlation between the swelling of these samples and the level of fluid absorption. The composites exhibited different levels of swelling depending on direction. These effects were well in line with the influence of fibres on restriction of the matrix deformation in the fibre direction. These differences correlated well with the average fibre orientation with respect to the various direction axes.

Introduction

Glass fibre reinforced polyamides, such as polyamide 6 and 66, are excellent composite materials in terms of their high levels of mechanical performance and temperature resistance. However, the mechanical properties of polyamide based composites decrease markedly upon absorption of water and other polar fluids. The mechanical performance of these composites in a hydrothermal environment results from a combination of the fibre and matrix properties and the ability to transfer stresses across the fibre-matrix interface.

Variables such as the fibre content, diameter, orientation and the interfacial strength are of prime importance to the final balance of properties exhibited by injection moulded thermoplastic composites [1-5]. Short fibre reinforced thermoplastics have been used in the automotive industry for many years and there has recently been a strong growth in the use of polyamide based materials in under-the-hood applications [6]. These applications place stringent requirements on such materials in terms of dimensional stability and mechanical, temperature and chemical resistance. There has been a rapid increase in the number of moulded composites exposed to engine coolant at high temperatures [7-10] and this has led to a need for an improvement in our understanding of the performance of glass-reinforced-polyamide under such conditions.

Typical testing for these applications involves measurement of mechanical properties before and after conditioning of the test material in model coolant fluids for a fixed time, up to 1000 hours, at temperatures in the 100-150°C range. It is not always easy to obtain a good understanding of the structure-performance relationships of a material from such snapshots of performance taken at a single condition. However, it has been known for sometime within the industry that the chemical nature of the glass fibre sizing can have a

strong influence on the retention of some mechanical properties of composites exposed to such hydrothermal conditioning. It is also well known that polyamide materials absorb relatively high levels of moisture when exposed to hydrothermal conditioning in water and that this can cause significant dimensional changes [11-17]. Despite this, and the fact that such hydrothermal testing has become commonplace for under-the-hood applications, there has been little systematic investigation of dimensional change of glass-fibre reinforced polyamide composites during such conditioning in coolant fluid. Thomason [17] has recently reviewed the mechanical performance and dimensional changes observed in glass fibre reinforced polyamide 66 during conditioning in coolant fluid at 120°C and 150°C. A rapid reduction was observed in both the modulus and strength of these composites and the matrix polymer in the initial stage of conditioning. However, unnotched impact was seen to initially increase significantly. Due to the rapid rate of fluid absorption and dimensional change at these high temperatures it was not possible to examine these effects in detail. This report presents the results of a further systematic study of the changes of dimension of injection moulded glass reinforced polyamide 66 composites during hydrothermal conditioning in model coolant fluid. Composites have been prepared using two chopped glass products where one contains a sizing system which has been optimised to improve the performance of composites subjected to hydrothermal treatments. To enable study of the initial stages of the process the conditioning temperature has been limited to 70°C for a range of conditioning times up to 400 hours. The data on the dimensional and weight changes are presented and discussed in this paper, the thermal and mechanical performance will be discussed elsewhere.

Experimental

The injection moulded polymer and composite bars for this study were supplied by the 3B fibreglass company. The polyamide 66 (PA66) used was DuPont Zytel 101. Composite samples with 30% weight fibre content were produced using this polymer and two chopped Advantex™ E-glass products. Advantex™ is a boron free E-glass formulation. These products were chopped to a length of 4 mm and the individual fibres had a nominal average diameter of 10 µm. Both samples were coated with sizings which are designed for polyamide reinforcement. DS1143 is a typical sizing designed to maximise the “dry as moulded” (DaM) performance of glass reinforced polyamides. The main ingredients of such sizings are typically aminosilane coupling agent and a commercial polyurethane dispersion [18,19]. DS1110 sizing contains some extra components which enhance the retention of composite mechanical properties in elevated temperature hydrolytic environments [20-22]. Three series of samples were moulded, series A using DS1143 glass, series B using DS1110 glass, and series R containing only the PA66 resin. The glass and polymer were compounded on a twin screw extruder and injection moulded to produce end-gated rectangular bars of with nominal dimensions 80x10x4 mm.

The test bars for this study were received vacuum packed in a DaM state. On removal from the packaging all samples were weighed and their three dimensions recorded at room temperature prior to conditioning. A micrometer with an operating range between 0-50mm ± 0.005mm was used in order to measure the width and the thickness of the test samples. It is well known that the cross section of injection moulded samples may not be exactly rectangular and it was noted that the recorded dimension varied slightly dependent on where the measurement was taken. To ensure consistency measurements were therefore taken at the

exact centre of each sample, as per ISO 179. The sample bars length exceeded the range of the micrometer and so the length of the test samples was measured using a vernier calliper with an accuracy of ± 0.01 mm was used. A digital balance with an operating range between 0-20 g ± 0.0001 g was used to measure sample weights. Each data point presented is the average of measurements on seven individual samples. Since these samples were subsequently used for impact testing this means that each data point for each conditioning time was obtained on a different set of seven samples. Hydrolysis conditioning took place in a temperature controlled bath with samples fully immersed in a 50:50 mixture of water and glycol at 70°C. Samples were stacked vertically and individually in a specially constructed rack such that the fluid had access to all surfaces of each sample. Conditioning times were chosen in the range 0-400 hrs. On removal from the conditioning container surface fluid was removed from the samples with tissue and then they were again weighed and their dimensions recorded. These samples were then equilibrated at room temperature in a 50:50 mixture of water and glycol for 24 hours after which they were again weighed and measured and then transferred immediately to the impact tester.

Results

Moisture absorption related processes in polymers and composites are normally analysed against the square root of exposure time to enable the use of standard diffusion models [12-17,23] and we have followed this procedure in the figures which are presented here. Error bars in these figures represent the 95% confidence interval on the average value. Figure 1 shows such a plot of percentage increase in sample weight of the injection moulded impact bars for composites A and B and the resin only sample after hydrolysis at 70°C and prior to the 24 hour cooling and equilibration step in the experimental procedure. The data appears

to show the main aspects typical of Fickian diffusion with a rapid initial uptake of liquid followed by a slow approach to an equilibrium absorption level. However, it is interesting to note that there does not appear to be a clear initial linear dependence of the weight increase as might be expected from a simple 1-D Fickian diffusion analysis [23].

It seems reasonable to assume that the glass fibres do not account for any of the weight increase seen during the hydrolysis treatment [12-17] and that the weight increase observed with the composites is solely due to weight changes of the polymer matrix. By dividing the composite weight increase by the average matrix content it is possible to examine the composite matrix weight change during these experiments. This data is also shown in Figure 1. It can be seen that at short conditioning times there is little significant difference in the level of fluid absorption between the composite matrices and the polymer sample. However at longer times (>24 hours) there is deviation from this trend and the composite matrices absorb significantly less fluid compared to the expectation based on the unreinforced polymer results. This has been previously observed to a greater degree in similar experiments carried out at higher temperatures and longer times [17]. Apparently the presence of the glass fibres reduces the ability of the polyamide matrix to absorb the same equilibrium level of fluid that is absorbed by the polymer in an unrestrained environment. It can also be seen in Figure 1 that there is no significant difference between the absorption results obtained with two composite systems A and B at this conditioning temperature.

The hydrolysis conditioning also resulted in significant changes in the dimensions of the polymer and composite samples. Although the sample dimensions were measured both on

removal from the 70°C conditioning bath and after the 24 hour equilibrium conditioning at 23°C, the high temperature dimensions are complicated by the dimensional change due to the increase in temperature as well as the swelling due to fluid absorption. For this reason only dimensional changes after the samples had equilibrated at 23°C will be considered here. The data are presented as percentage change in thickness, width and length in Figures 2-4. The results for the change in thickness and width of the injection moulded bars as a function of conditioning time are shown in Figures 2 and 3. The curves in Figure 2 for sample thickness follow similar trends as the weight increase data in Figure 1. Interestingly, in the early stages of conditioning there is little significant difference in the thickness increase observed in the composites and the polymer samples despite the fact that the presence of the glass fibres lowered the relative fluid uptake of the composites compared to the polymer. At longer conditioning times the polymer does appear to increase in thickness more than the composites but still not in the relative proportions observed in Figure 1. It can further be noted from Figures 2 and 3 that the thickness of the composite samples appears to increase significantly more than the width. Despite the reduced level of change in the samples width it can be seen that the polymer sample exhibits a greater change in width than the composites across the full range of conditioning experiments. In Figure 4 the data on the sample length exhibit some very different relative trends. The polymer still shows an increase in length dimension with increasing conditioning time although at a significantly lower level than the thickness or width. However, the composite samples exhibit only a minimal change in length across the range of conditioning times achieving only a 0.3% increase in length after the maximum 400 hours conditioning. When comparing the results in Figures 2-4 it is notable that the confidence limits on the thickness results are significantly greater than those for width and length of the sample bars. This is

likely caused by a combination of the relative error calculation where the divisor is smallest for the bar thickness and the deviations in sample cross section caused by shrinkage during cooling in the injection moulding process. Figure 5 shows a cross section of a system A bar. It can be seen that there is visible curvature in the upper and lower surfaces due to shrinkage. This curvature was more notable in the composite samples. This is likely due to the fibre orientation in these composite moulded bars (see later discussion) which resists the shrinkage more in the length and width directions and consequently, though Poisson's effects, enhances the shrinkage in the thickness direction. Although the sample thickness was always measured at the centre of each bar this curvature does add an extra sample to sample variability and consequently increase the confidence limits on the average value. It is noted that the average confidence limit on the sample thickness was 50-60% less for the polymer bars (with less visible surface curvature) than the two composite systems.

Discussion

In fluid absorption experiments in polymers, plate-shaped samples are generally preferred so that the fluid absorption is mainly determined by the uptake through the two broad faces of the plate. In this situation diffusion is approximated to occur in one direction only. Consequently, if fluid uptake is determined by classical Fickian diffusion, the fluid concentration can be approximated by the well known solution for diffusion in an infinite plate, which yields a linear increase in the weight increase of the sample with $t^{1/2}$ over the initial part of the experiment. However, when samples with different shapes are employed then corrections have to be made for edge effects where the sample weight is also increased by fluid uptake via the other available surfaces of a rectangular specimen. Correction factors for such edge effects have been derived and have been used in many publications on

moisture absorption [24-27]. If moisture uptake is determined by classical 1D Fickian diffusion, for diffusion in an infinite plate the moisture concentration then the mass of fluid adsorbed in time t , $M(t)$, as a fraction of the final equilibrium of M_e is given by

$$\frac{M(t)}{M_e} = 1 - \frac{8}{\pi^2} \sum_{n=0}^{\infty} (2n+1)^{-2} \exp\left[-(2n+1)^2 \left(\frac{\pi^2 D_x t}{a^2}\right)\right] \quad (1)$$

Where D_x is the diffusivity in the x direction and a is the thickness in the x direction.

When $D_x t \ll 0.05a^2$ equation 1 can be reduced to

$$\frac{M(t)}{M_e} = \frac{4}{\pi^{1/2}} \left(\frac{D_x t}{a^2}\right)^{1/2} \quad (2)$$

And thus the diffusivity can be obtained from the initial linear portion of the absorption curve and the final equilibrium absorption level. In the case of fluid adsorption into a real 3-dimensional monolithic rectangular of dimensions a, b, c in the x, y, z directions where $D_c = D_x = D_y = D_z$ Starink [27] showed that an edge correction factor f could be introduced into equation 1 to give the effective diffusion coefficient

$$D_{eff} = f^2 D_c \quad (3)$$

$$f = 1 + 0.54 \frac{a}{b} + 0.54 \frac{a}{c} + 0.33 \frac{a^2}{bc} \quad (4)$$

Using the dimensions a, b, c of the samples in this study results in a value of $f=1.212$. It was clearly showed [27] that the effect of the edge correction factor is to induce a positive curvature into the initial linear portion of the absorption similar to that observed in the data in Figure 1. Using the above analysis and the initial slopes taken from the first data points in Figure 1 results in values of $D_{eff} = 12.0 \times 10^{-12} \text{ m}^2/\text{s}$ for the PA66 polymer and $10.4 \times 10^{-12} \text{ m}^2/\text{s}$ for the composites, which is in reasonable agreement with the values reported by Ishak and Berry [12]. However, given the apparent curvature of lines in Figure 1 it was also decided to fit the full curves using equation 1. The results of this exercise are shown in

Figure 6. It can be seen that the values of D_{eff} given above are only a good fit for the early part of the absorption curve. A better fit over a greater proportion of the curve is obtained using a value of $D_{\text{eff}}=5.3 \times 10^{-12} \text{ m}^2/\text{s}$ or $D_c=3.6 \times 10^{-12} \text{ m}^2/\text{s}$ for both polymer and composites. However, it can clearly be seen in Figure 6 that the initial stage of the absorption process appears to require a higher value of D_{eff} . There are numerous documented sorption anomalies from the standard Fickian case, the anomalously short initial linear portion exhibited by the sorption curves in Figure 6 is normally referred to as Pseudo-Fickian behaviour [28].

Sorption and transport in polymers with long relaxation times often exhibit features which cannot be described adequately by any generalised form of Fick's law. This non-Fickian behaviour is usually observed with glassy polymers and semicrystalline polymers above their glass transition temperature (T_g). The T_g of the PA66 matrix is reduced well below the conditioning temperature due to the absorption of fluid [17]. In such cases D may be a function of concentration or time or both [28]. This type of anomalous behaviour can be characterised experimentally determining the time dependence of the weight increase of the samples under conditioning. This pseudo-Fickian behaviour is further confirmed in Figure 7 which is a plot of $\log M(t)$ against \log time. Fickian sorption would give a line with slope 0.5 in this Figure whereas slopes <0.5 are characteristic of pseudo-Fickian behaviour. It can be seen that a slope of approximately 0.36 is obtained for the unreinforced polymer and both composite systems. As discussed above, this type of behaviour can often be explained by the use of a time dependent diffusion coefficient. By adjusting the value of D_{eff} input into equation 1 between the two extremes reported above it is possible a much improved fit to the experimental data as shown in Figure 8. Figure 8 also shows the values of D_{eff} used in

these calculations. Figure 8 implies D_{eff} is high in the initial stages of moisture absorption but decreases rapidly to a constant value as the conditioning time increases. Interestingly Figure 9 shows a similar analysis for previously published data [17] obtained on water:glycol conditioning of the same materials at 120°C. The required form of D_{eff} versus time is clearly similar to that obtained in this work. The question is whether the suggestion of such a time dependent diffusion coefficient is realistic.

During the injection moulding process molten polymer is forced at high pressure into temperature controlled moulds. This process results in a layered structure, a thin, quenched and virtually amorphous surface layer, a relatively high crystallinity, slow cooled core, and a less crystalline transition layer [29]. Depending on the moulding conditions, in particular melt temperature, mould temperature and moulding thickness, the demoulded material may consist entirely of the surface and transition layers [29]. After initial crystallization, nylons can undergo further secondary crystallization. Generally, the lower the initial level of crystallinity and the higher the level of absorbed water, the higher will be the rate of secondary crystallization at any given temperature [30]. It is generally accepted that moisture diffuses into the polymer via the non-crystalline volume and therefore the D_{eff} can be expected to be inversely dependent on the local crystallinity of the polymer or composite matrix. Illers studied the effects of temperature and moisture conditioning on the density and thermal properties of quenched PA66 films [31]. He reported a 0.5% density increase in density of quenched PA66 films after 10 days water immersion at room temperature. Equilibrium moisture uptake was achieved after 6 months and resulted in a total density increase of 2.14%. Quenched PA66 was reported to have a pseudohexagonal crystal structure which was converted to triclinic when annealed above 180°C. A linearly

decreasing relationship between equilibrium moisture uptake and polymer crystallinity was also observed. It was noted that equilibrium moisture uptake was dependent on the total level of crystallinity. However, equilibrium moisture uptake at equal crystallinity was reduced after high temperature annealing. A detailed study of the structure and morphology of injection moulded PA6 [29] revealed the three layer structure with a low density surface layer transitioning to a higher density core. This profile was reversed by boiling water conditioning resulting in an overall increase the density of the moulded bars with a higher density in the conditioned surface layer compared to the core. A tribological study of injection moulded PA66 also reported that different microstructures were obtained by altering the mould temperatures in the injection moulding process [32]. A cross-section of the samples showed a non-spherulitic skin followed by a transition region and a spherulitic core. A clear difference in spherulite size was observed dependent on mould temperature. In general the higher the mould temperature used, the bigger the average spherulite size. In summary, many investigations of injection moulded nylons have confirmed this layered structure in many types of polyamides including PA6 and PA66. It has been shown that the structure and crystallinity in the surface and transition layers can be radically altered by conditioning at elevated temperature and that these changes are accelerated in the presence of moisture. In particular moisture conditioning has been shown to invert the crystallinity profile in the cross section of these moulded samples resulting in a higher than average crystallinity in the surface layers after conditioning. It should be noted that another result of this annealing is an increase in the density of the samples despite the fact that the absorbed moisture has a lower density than the dry polyamide.

Figure 10 shows the change in the density of the PA66 polymer samples over the time of the conditioning experiments. It can be seen clearly that, despite the fact that the density of the conditioning fluid is lower than that of PA66, there is a step increase in polymer density of approximately 0.9% at the beginning of the experiment. After this initial step change there is a continuous gradual increase in density with conditioning time up to approximately 1.4%. These values are well in line with other published values of density change in PA66 due to hydrothermal annealing [29,33]. The density values (ρ) can be converted into average crystallinity values using

$$X_c = \frac{\rho - \rho_a}{\rho_c - \rho_a} \quad (5)$$

Where $\rho_a=1.08$ and $\rho_c=1.24$ for amorphous and fully crystalline PA66 [29,34]. These data are also shown in Figure 10. The inverse relationship between diffusion coefficient and polymer crystallinity is apparent from comparison of Figures 8 and 10 and is further confirmed by direct comparison of these two parameters in Figure 11. It should be noted that the values for crystallinity given here are averages across the sample. Assuming that the normal three layer structure is present in these injection moulded samples then during the conditioning process it follows that the initial fluid uptake will be dominated by the surface layer of the samples. Given that the surface layer is quenched and virtually amorphous then it also follows that a high value of D_{eff} would be observed at this stage. As the surface layer rapidly reaches equilibrium fluid uptake the average D_{eff} will drop as the absorption process becomes more dependent on the higher crystallinity transition region and core. Simultaneously, the surface layer crystallinity will increase due to annealing effects which also proceed rapidly due to the elevated temperature and high moisture conditions at

and near the surface. This increase in crystallinity will lead to a further lowering of the average value of D_{eff} for the sample and a greater level of change of D_{eff} with time.

From the above analysis it would seem that there is a good case to be made for a time dependent diffusion coefficient related to changes in crystallinity (and possibly crystal structure) due to hydrothermal annealing of the initial non-equilibrium structure of the injection moulded PA66 as the explanation for the deviations from simple Fickian diffusion observed in the absorption versus time data presented in Figure 6.

Further to the changes in mass due to fluid absorption and changes in volume due to annealing it is also of interest to analyse changes in sample dimensions due to swelling. The elastic behaviour of composite materials is often considered in terms of deformations caused by mechanical stresses due to physically applied loads. However, deformations are also produced by environmental changes such as temperature changes and moisture absorption. The relevant physical parameters which quantify these phenomena are the coefficients of thermal expansion (CTE) and the coefficients of swelling. Although CTE's are the more familiar of these coefficients, these two phenomena are similar and can be treated in a similar fashion. The swelling coefficient (β) is defined as $\beta = \epsilon / C$ where $\epsilon = \delta L / L$ the swelling strain in any direction and $C = \delta W / W$ the mass of absorbed moisture per unit mass [17,35].

Figure 12 shows the values for the volumetric swelling $\epsilon_v = \delta V / V$ versus C for the composites and PA66 polymer. It can be seen that excellent linear relationships are obtained for the change in dimensions for both composite and polymer samples. It is

interesting to note the least squares fitted lines in Figure 12 do not pass through the origin but intersect the $C=0$ axis at approximately -0.7% to -0.9%. This is further evidence for the step change in density of the polymer and composite matrix early on in the conditioning process and these values are a good match to the value of the step density change (0.9%) obtained in Figure 10. It is relatively trivial to show that, if the polymer or the composite matrix swells by the volume of the absorbed liquid then a value of $\beta = \rho_R / \rho_A$ is obtained for the slope of the lines in Figure 12 where ρ_R and ρ_A are the densities of the polyamide resin and absorbed fluid. Although we cannot be sure that the polymer absorbs fluid containing the same ratio of water/glycol as is present in the treatment bath, by using a value of $\rho_A = 1.07$ an expected slope = 1.045 is obtained. Given the uncertainty introduced by the post crystallisation of the matrix due to the annealing effects of the conditioning it can be stated that within the experimental error the dimensional change of the polyamide resin is exactly explained by the simple change in mass and volume due to the amount of fluid which the sample absorbs.

Figures 13-15 presents the results for the linear swelling coefficients in the thickness, width and length directions of the three samples in this study. It is clear from these figures that the volumetric swelling shown in Figure 12 is not equally divided in the three sample dimensions. The solid lines in Figure 13-15 are the least squares fitted lines for the data and from the slope of these lines we obtain values of β summarized in Table 1. The directional dependence of CTE's in fibre reinforced composites is well known and is attributed to the restriction of expansion in the fibre direction due to the much lower CTE of the fibre compared to the polymer matrix [17,36,37]. In a similar fashion it can be assumed that $\beta=0$ for glass fibres and so the presence of fibres will restrict the swelling in the fibre direction

and consequently increase the swell normal to the fibre direction due to Poisson's effects in the matrix. There is little degree of out of plane fibre orientation (through the thickness) in these injection moulded samples and consequently we observe a higher swell in the thickness as compared to the width where the fibres in the "core" of the moulding have a somewhat more random in-plane orientation. Since the highest level of fibre orientation is in the flow direction in the mould, very low levels of swell in the length direction of the composite samples can be expected. It can be seen from the values of β in Table 1 that these expectations are borne out in the data. It is interesting to note in Table 1 that some directional dependent differences are also observed in the β values for the moulded PA66 polymer resin samples. This may well be indicative of some orientation at the molecular level in the injection moulded polyamide polymer. Thomason has previously published values for the fibre orientation parameter in the length, width and thickness directions in injection moulded glass reinforced PA66 bars of very similar dimensions to the samples in this study [38]. Figure 16 shows the values of β from the composites in this study plotted against those values of orientation parameter. It can be seen that a good inverse linear correlation is obtained between these two data sets. This would appear to give strong support to the above explanation of the direction dependent swelling observed in these composites.

Conclusions

This study of injection moulded glass-fibre reinforced polyamide 66 composites has revealed that hydrothermal conditioning in water-glycol mixtures results in significant changes in the weight and dimensions of these materials. All materials showed a weight increase due to hydrothermal conditioning at 70°C which was typical of a pseudo-Fickian diffusion process. It was noted that the presence of the glass fibres reduced the fluid uptake by an amount significantly greater than would be expected from a simple scaling with the polymer content of the composites. The weight changes of the polymer and composite samples could be well modelled by a Fickian diffusion process with a time dependent diffusion coefficient. It was proposed that this time dependent diffusion coefficient was related to the presence of a quenched layer on the surface of these injection moulded samples. A strong correlation was observed between the swelling of these samples and the level of fluid adsorption. It was not apparent that changing the glass fibre sizing affected the dimensional stability of the composites. Although the PA66 resin showed reasonably homogeneous swelling, the composites exhibited different levels of swelling depending on direction. These effects were well in line with the known effects of fibres on restriction of the matrix deformation (mechanical, thermal or moisture swelling) in the fibre direction. These differences could be well correlated with the average fibre orientation with respect to the various direction axes.

Acknowledgement

The author gratefully acknowledges the support of 3B Fibreglass, Battice, Belgium with the preparation and moulding of the materials used in this study.

Tables

	Swelling Coefficients			
	Volume	Thickness	Width	Length
PA66 Polymer	0.94	0.33	0.30	0.28
System A	1.04	0.52	0.44	0.06
System B	1.00	0.49	0.43	0.06

Table 1: Swelling coefficients of moulded PA66 polymer and Composites

References

1. Sato N, Kurauchi T, Sato S, and Kamigaito O. Reinforcing mechanism by small diameter fiber in short fiber composites. *J. Compos. Mater.* 1998;22:850-873
2. Hassan A, Yahya R, Yahaya AH, Tahir ARM, Hornsby PR. Tensile, Impact and Fiber Length Properties of Injection-molded Short and Long Glass Fiber-reinforced Polyamide 6,6 Composites. *J.Reinforced Plastics and Composites* 2004;23:969-986.
3. Thomason JL. Structure-property relationships in glass reinforced polyamide: 1) The effect of fibre content. *Polym.Composites* 2006;27:552-562.
4. Thomason JL. Structure-property relationships in glass reinforced polyamide: 2) The effects of average fibre diameter and diameter distribution. *Polym.Composites* 2007;27:331-343.
5. Mouhmid B, Imad A, Benseddiq N, Benmedakhène S, Maazouz A. A study of the mechanical behaviour of a glass fibre reinforced polyamide 6,6. *Polymer Testing* 2006;25:544-552.
6. Carlson E, Nelson K. Nylon under the hood: history of innovation. *Automotive Engineering* 1996;104:84-89.
7. Harrison AR. Automotive Composite Components, Chapter 11 in *Integrated Design and Manufacture Using Fibre-reinforced Polymeric Composites*. Eds. Owen MJ. Middleton V. Woodhead Publishing, 2000.
8. Rudd CD. Composites for Automotive Applications, *Rapra Review Reports Volume 11, number 6, 2000, page 12*. Published by iSmithers Rapra, 2001
9. Page IB. Polyamides As Engineering Thermoplastic Materials. *Rapra Review Reports Volume 11, number 1, 2000, page 13*. Published by iSmithers Rapra, 2001.

10. Maxwell J. *Plastics in the Automotive Industry*. Pages 122-127. Society of Automotive Engineers. Published by Woodhead Publishing, 1994
11. Valentin D, Paray F, Guetta B. The Hygrothermal Behaviour of Glass Fibre Reinforced Pa66: a study of the effect of water absorption on their mechanical properties. *J.Mater.Sci.* 1987;22:46-56.
12. Mohd Ishak ZA, Berry JP. Hygrothermal Aging Studies of Short Carbon Fiber Reinforced Nylon 6.6. *J.Appl.Polym.Sci.* 1991;54:2145-2155.
13. Takeda N, Song D, Nakata K. Effects of temperature and water content on impact properties on injection-molded glass nylon-6 composites . *Adv. Composite Mater.* 1996;5:201-212.
14. Bergeret A, Pires I, Foulc MP, Abadie B, Ferry L, Crespy A. The hygrothermal behaviour of glass fibre reinforced thermoplastic composites. *Polym Testing* 2001;20:753-763.
15. Jia N, Fraenkel HA, Kagan VA. Effects of moisture conditioning methods on mechanical properties of injection molded nylon 6. *J.Reinforced Plastics and Composites* 2004;23:729-737.
16. I. Carrascal, J.A. Casado, J.A. Polanco, F. Gutiérrez-Solana, Absorption and diffusion of humidity in fiberglass-reinforced polyamide. *Polymer Composites* 2005;26:580-586.
17. Thomason JL. Structure-property relationships in glass reinforced polyamide: 3) Effects of hydrolysis ageing on the dimensional stability and performance of short glass-fibre reinforced Polyamide 66. *Polym.Composites* 2007;27:344-354.
18. Coakley TA, Rubadue JE, Forman CE, Schweizer RA. Non-discoloring glass strand size. United States Patent 4,255,317 (1981)

19. Thomason JL, Adzima LJ. Sizing up the interface: an insider's guide to the science of science. *Composites Part A* 2001;32:313-321.
20. Cossement M, Masson N, Piret W. Size composition. United States Patent 5,236,982 (1993)
21. Masson N, Henrion JM, Thomason JL, Adzima LJ, Cheney TL, Piret W, Cossement M. System for preparing glass fiber pellets having low discoloration. United States Patent 6,365,272 (2002)
22. Cossement M, Henrion JM. Two-part sizing composition for reinforcement fibers Patent United States Patent Application 20070154697 (2007)
23. Crank J, Park GS. (eds) *Diffusion in Polymers*, Academic Press, New York, 1968
24. Shen CH, Springer GS. Moisture absorption and desorption of composite materials. *J. Comp. Mater.* 1976;10:2-20.
25. Aronhime MT, Neumann S, Marom G. The anisotropic diffusion of water in Kevlar-epoxy composites. *J. Mater. Sci.* 1987;22:2435-2446.
26. Shanahan MER, Auriac Y. Water absorption and leaching effects in cellulose diacetate. *Polymer* 1998;39:1155-1164.
27. Starink MJ, Starink LMP, Chambers AR. Moisture uptake in monolithic and composite materials: edge correction for rectangularoid samples. *J.Mater.Sci.* 2002;37:287-294.
28. Rogers CE. 'Permeation of Gases and Vapours in Polymers' Chapter 2 in *Polymer Permeability*, ed. J Coymn, Elsevier Applied Science Publishers, London, 1985
29. Russell DP, Beaumont PWR. Structure and properties of injection-moulded nylon-6, Part 1: Structure and morphology of nylon-6. *Journal of Materials Science* 1980;15:197-207.

30. Xenopoulos A, Clark ES. Physical Structure In: Kohan MI, editor. Nylon Plastics Handbook. Munich: Hanser, 1995. p.108-136.
31. Illers KH. Dynamic mechanical behavior of drawn nylon 66 and poly(ethylene terephthalate) Colloid & Polymer Science 1975;253: 329-331.
32. Apichartpattanasiri S, Hay JN, Kukureka SN. A study of the tribological behaviour of polyamide 66 with varying injection-moulding parameters. Wear 2001;251:1557–1566.
33. Starkweather HW. The sorption of water by nylons. J.Appl.Polym.Sci. 1959;2:129-133.
34. Starkweather HW, Moore GE, Hansen JE, Roder TM, Brooi RE. Effect of crystallinity on the properties of Nylons. J.Polym.Sci. 1956;22:189-204.
35. Rosen BW. in Engineered Materials Handbook, Volume 1 Composites, ASM International, 1987
36. Schapery RA. Thermal Expansion Coefficients of Composite Materials Based on Energy Principles. J.Composite Materials 1968;2:380-390.
37. Thomason JL, Groenewoud WM. The influence of fibre length and concentration on the properties of glass fibre reinforced polypropylene: 2) Thermal properties. Composites 1996;27A:555-656.
38. Thomason JL. Micromechanical Parameters from Macromechanical Measurements on Glass Reinforced Polyamide 6,6. Compos.Sci.Technol. 2001;6:2007-16.

List of Figures

Figure 1 Weight gain of polymer, composite, and composite matrix versus conditioning time at 70°C

Figure 2 Change in sample thickness after conditioning at 70°C and equilibration at 23°C

Figure 3 Change in sample width after conditioning at 70°C and equilibration at 23°C

Figure 4 Change in sample length after conditioning at 70°C and equilibration at 23°C

Figure 5 Cross section view of composite bar system A

Figure 6 Fickian analysis of sample weight gain

Figure 7 Pseudo-Fickian analysis of sample weight gain

Figure 8 Fitting of time dependent diffusion coefficient (70°C data this study)

Figure 9 Fitting of time dependent diffusion coefficient (120°C data ref 17)

Figure 10 Polymer density and calculated crystallinity versus conditioning time

Figure 11 Diffusion coefficient versus polymer crystallinity

Figure 12 Volume change versus weight increase

Figure 13 Directional swelling coefficients for composite system A

Figure 14 Directional swelling coefficients for composite system B

Figure 15 Directional swelling coefficients for polyamide 66

Figure 16 Relationship of composite directional swelling coefficients and the fibre orientation parameters.

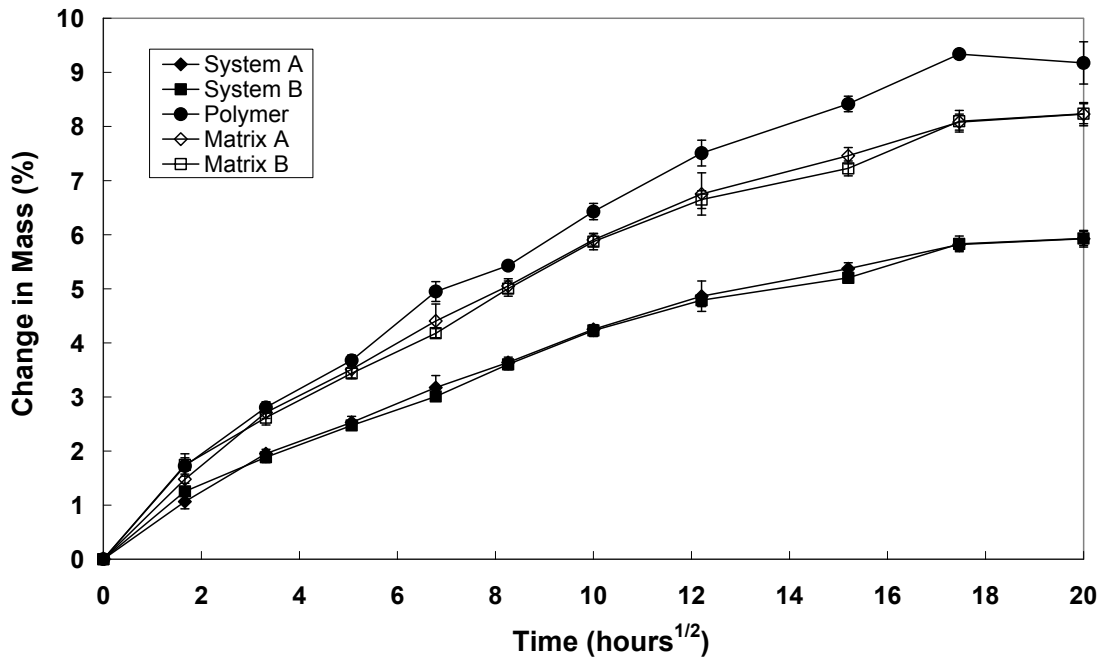


Figure 1 Weight gain of polymer, composite, and composite matrix versus conditioning time at 70°C

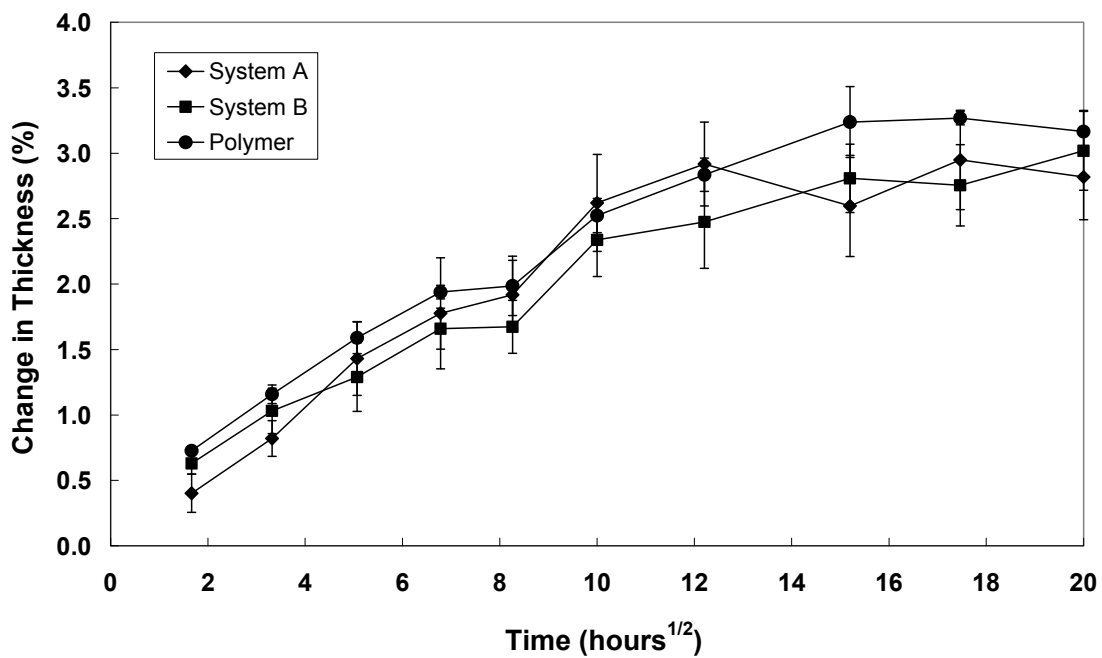


Figure 2 Change in sample thickness after conditioning at 70°C and equilibration at 23°C

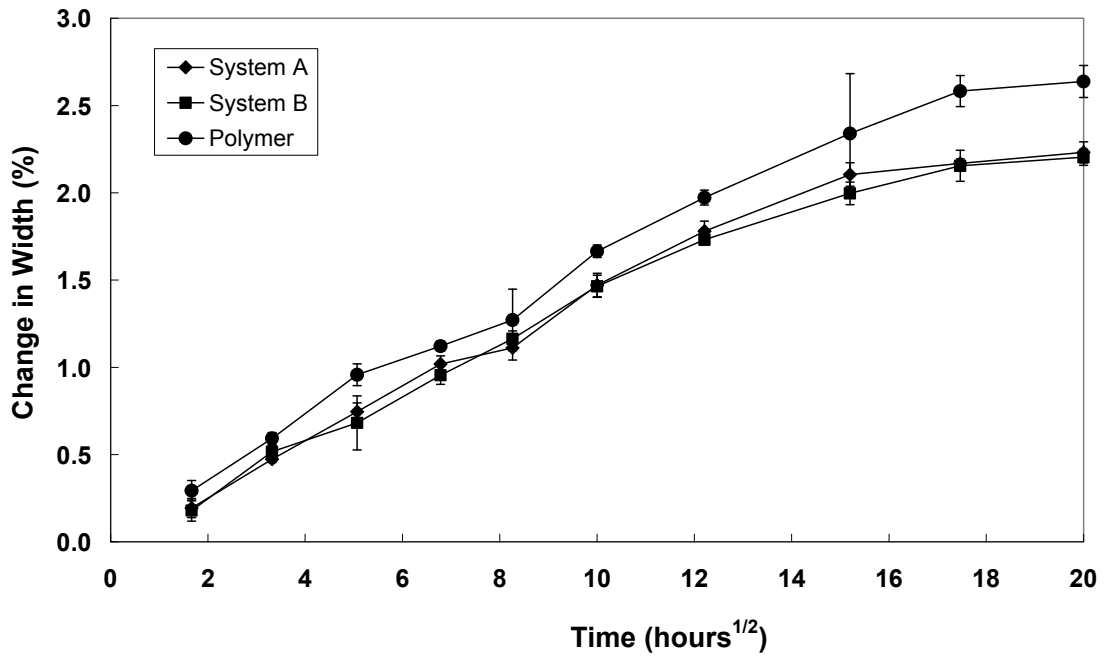


Figure 3 Change in sample width after conditioning at 70°C and equilibration at 23°C

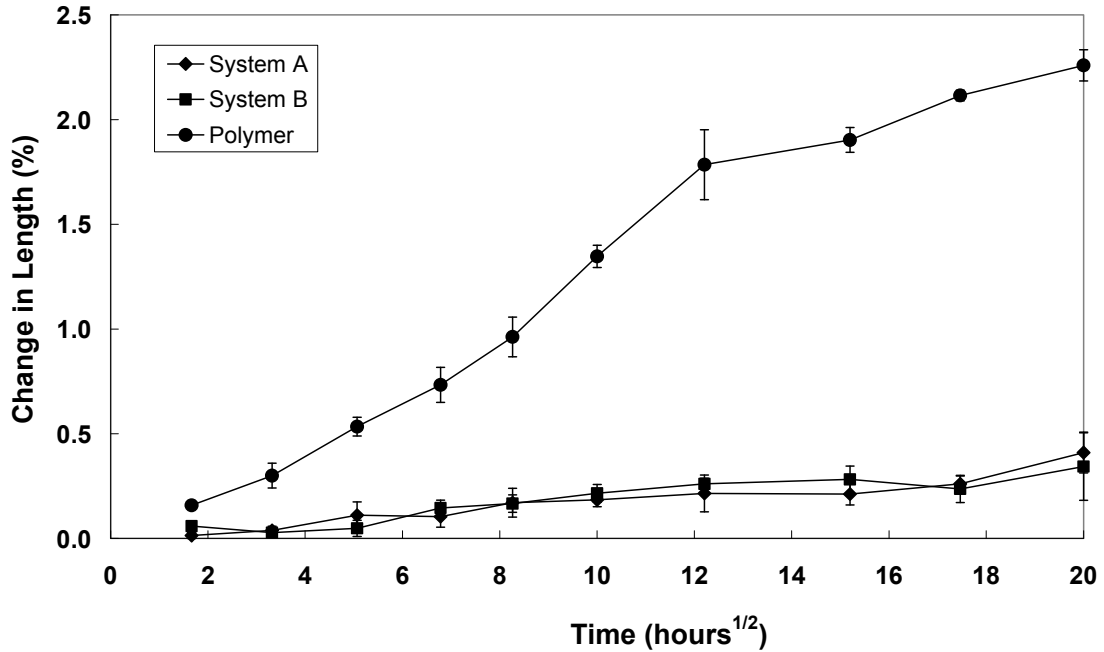


Figure 4 Change in sample length after conditioning at 70°C and equilibration at 23°C

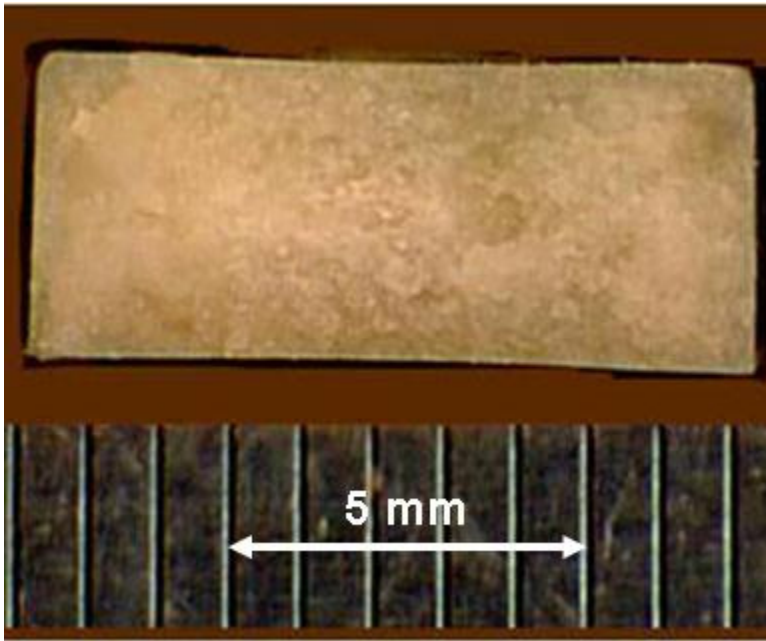


Figure 5 Cross section view of composite bar system A

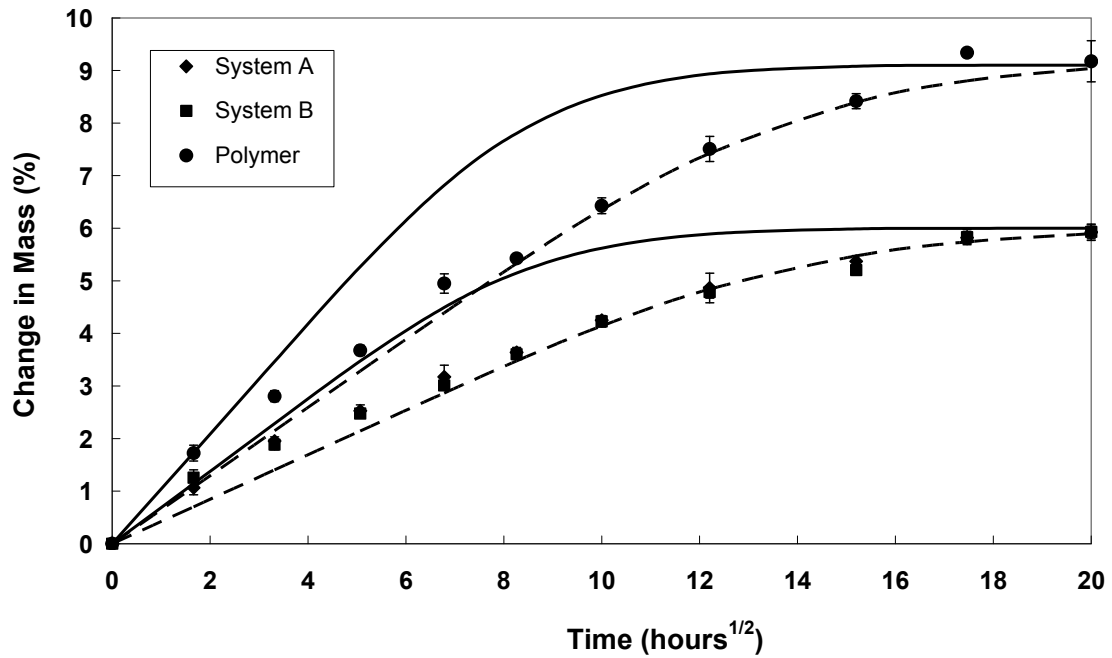


Figure 6 Fickian analysis of sample weight gain

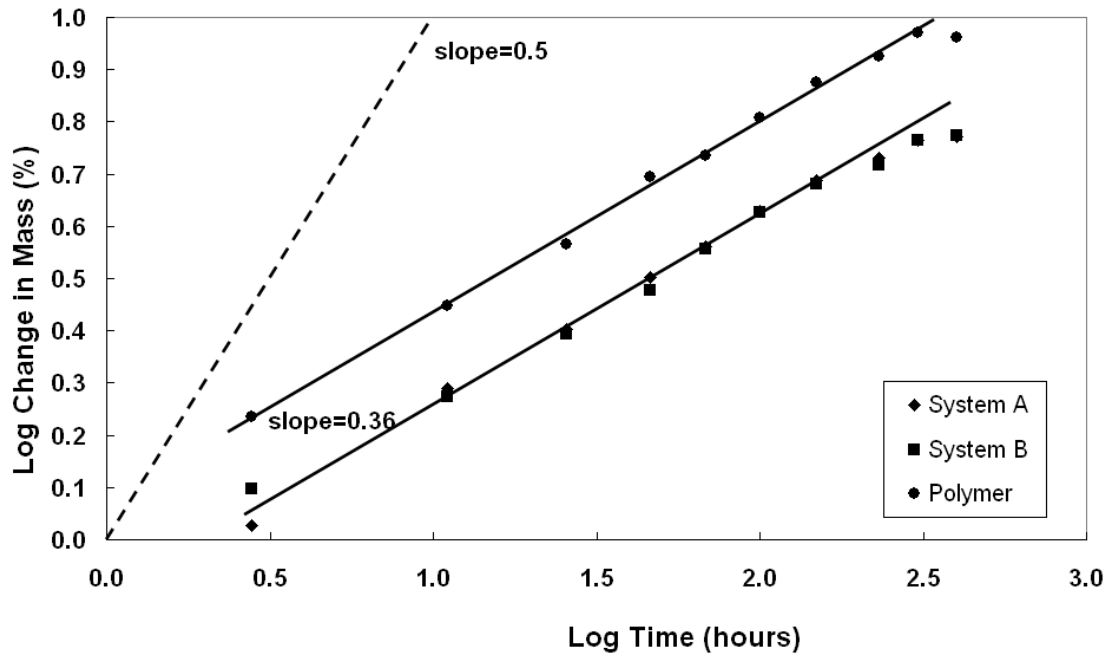


Figure 7 Pseudo- Fickian analysis of sample weight gain

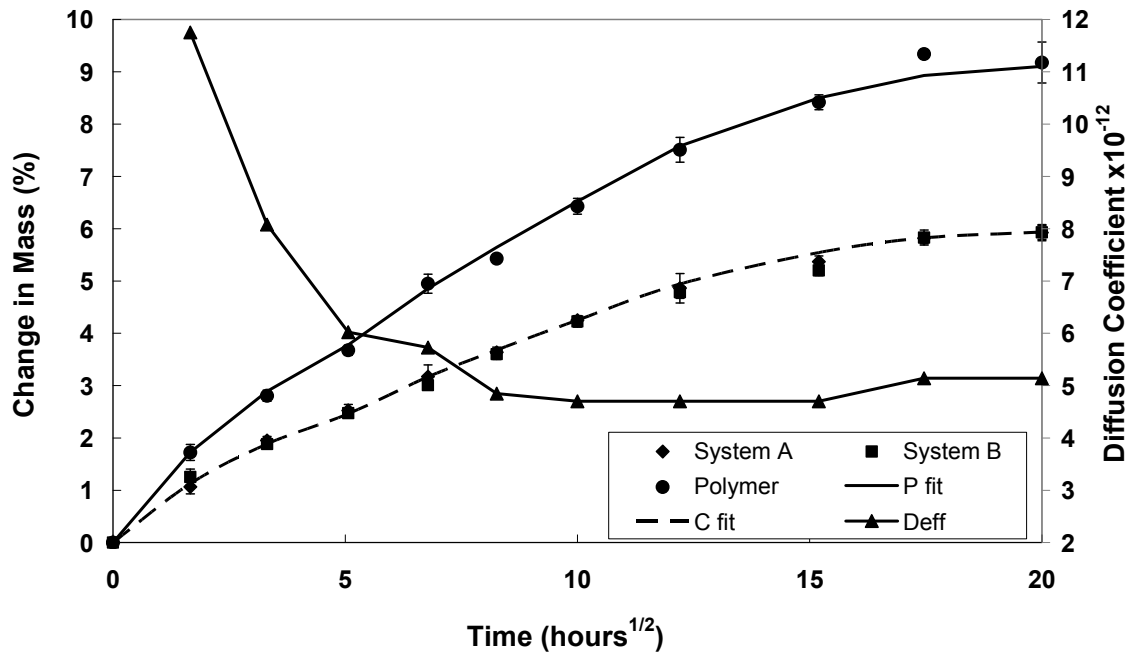


Figure 8 Fitting of time dependent diffusion coefficient (70°C data this study)

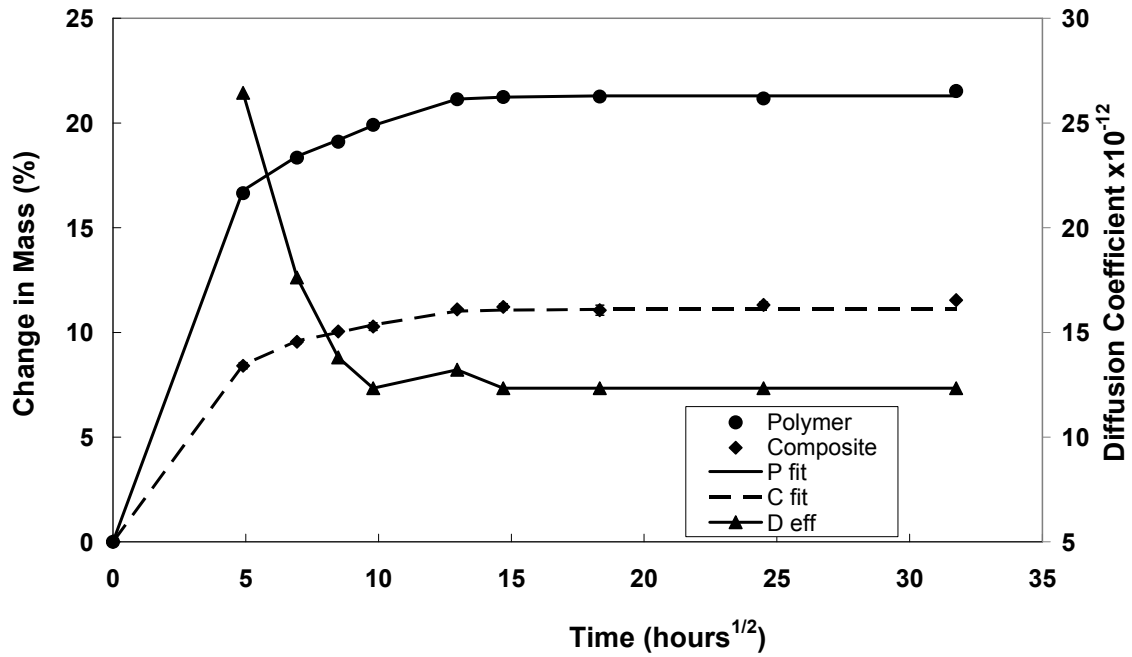


Figure 9 Fitting of time dependent diffusion coefficient (120°C data ref 17)

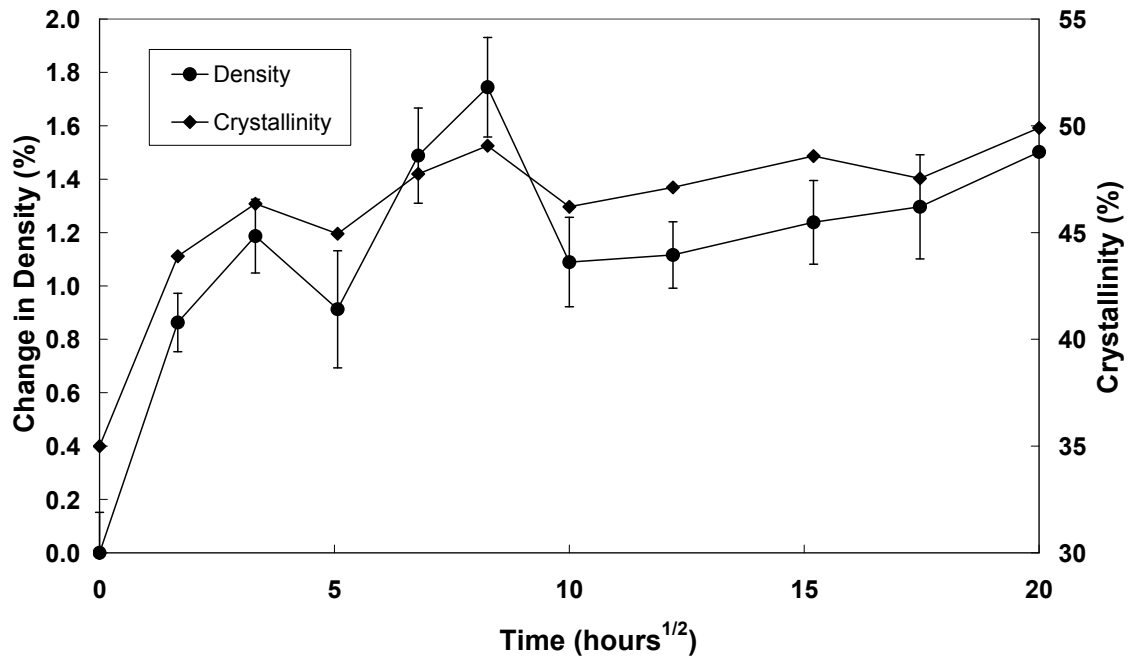


Figure 10 Polymer density and calculated crystallinity versus conditioning time

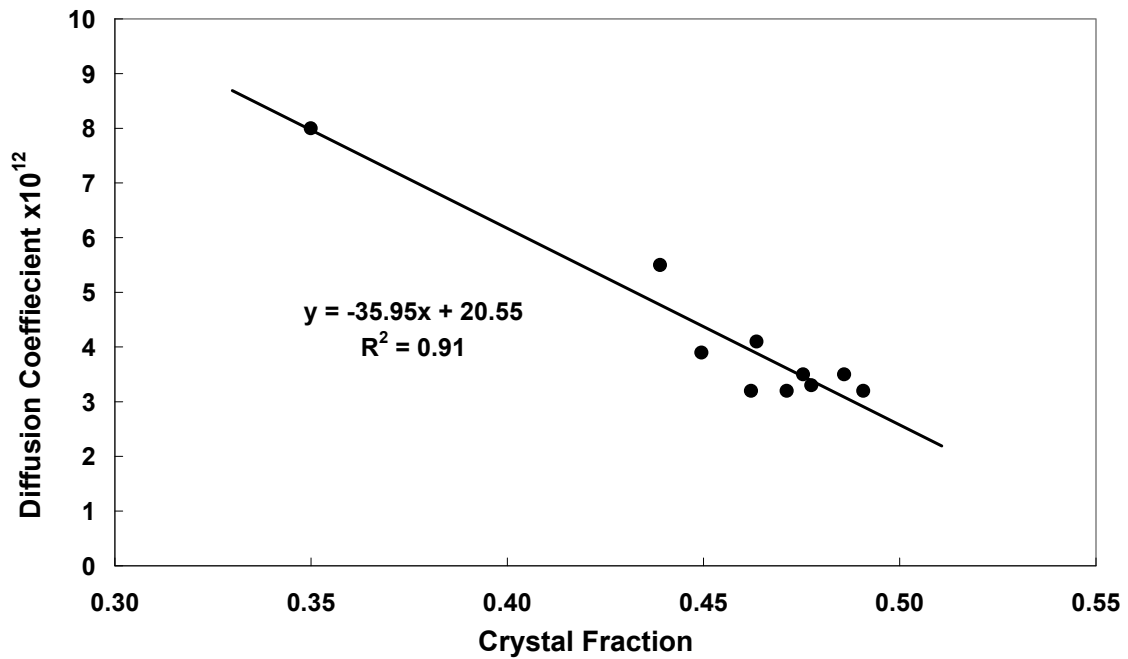


Figure 11 Diffusion coefficients versus polymer crystallinity

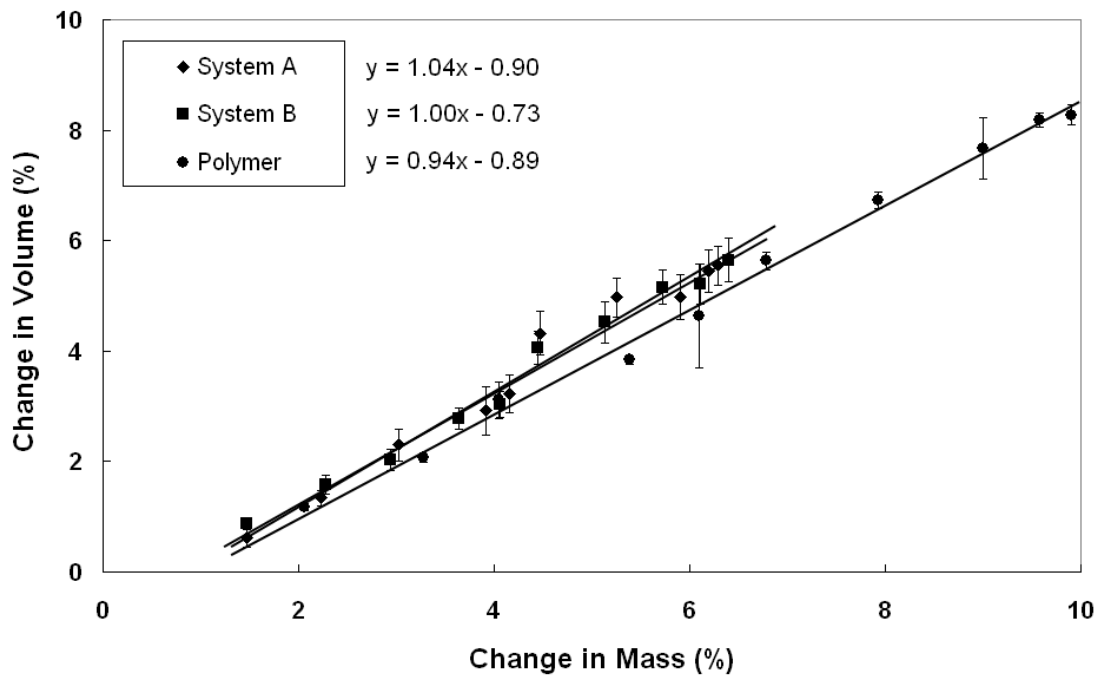


Figure 12 Volume change versus weight increase

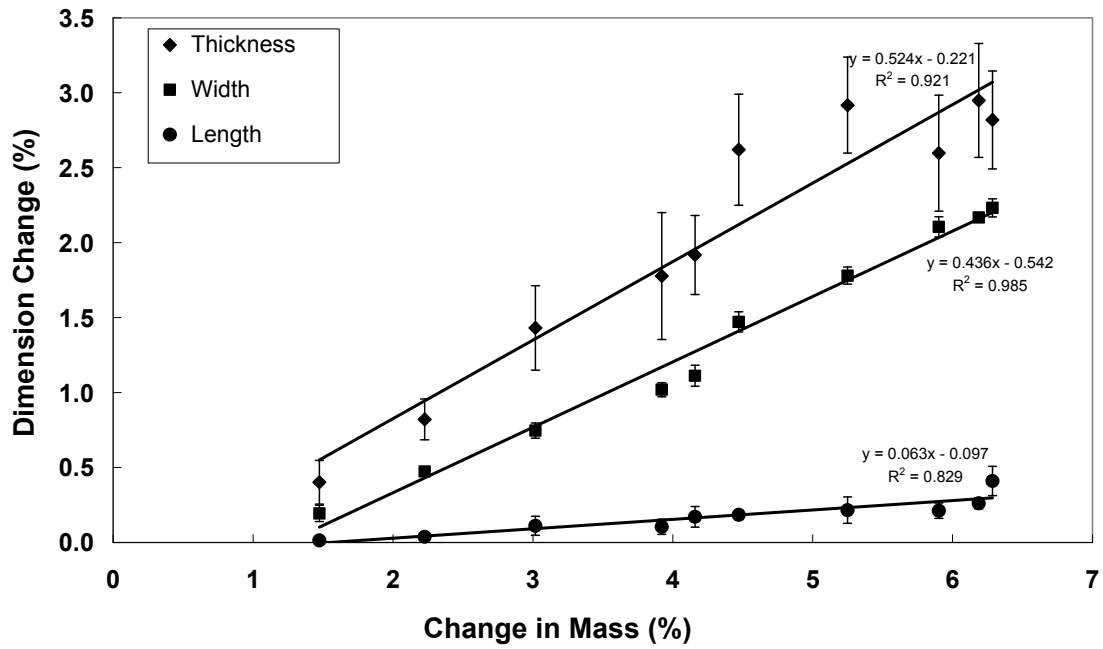


Figure 13 Directional swelling coefficients for composite system A

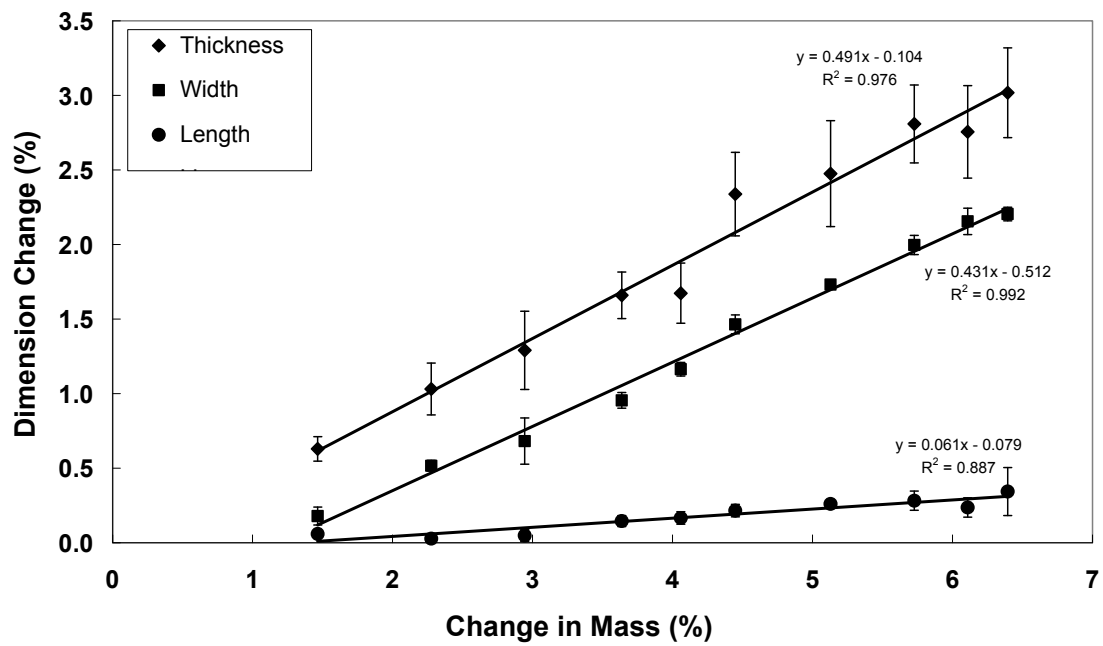


Figure 14 Directional swelling coefficients for composite system B

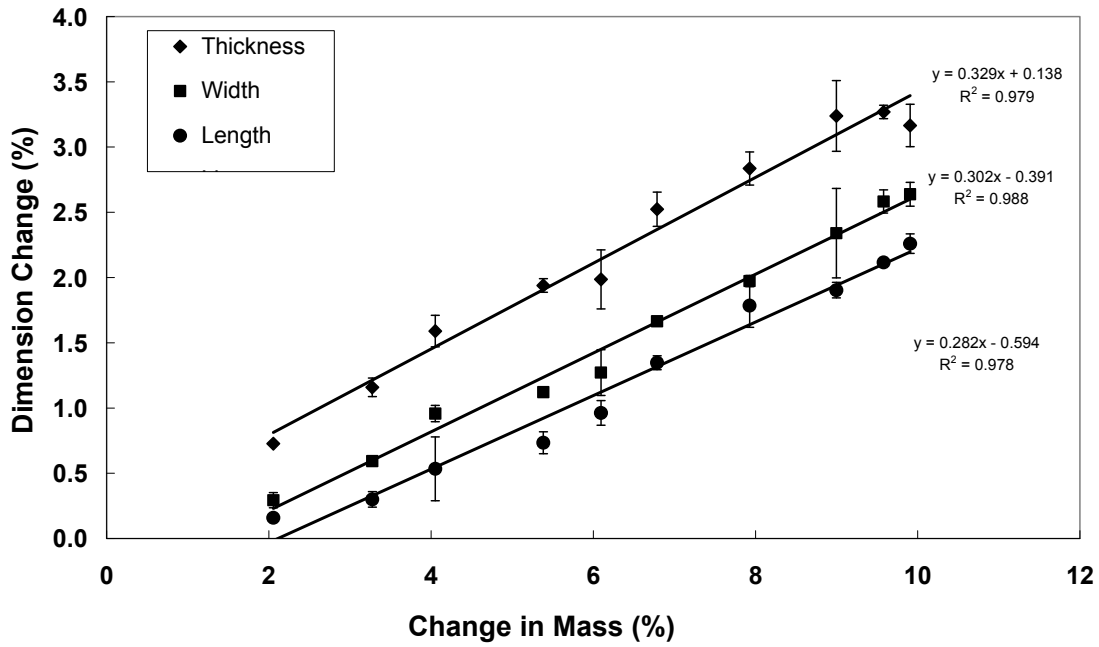


Figure15 Directional swelling coefficients for polyamide 66

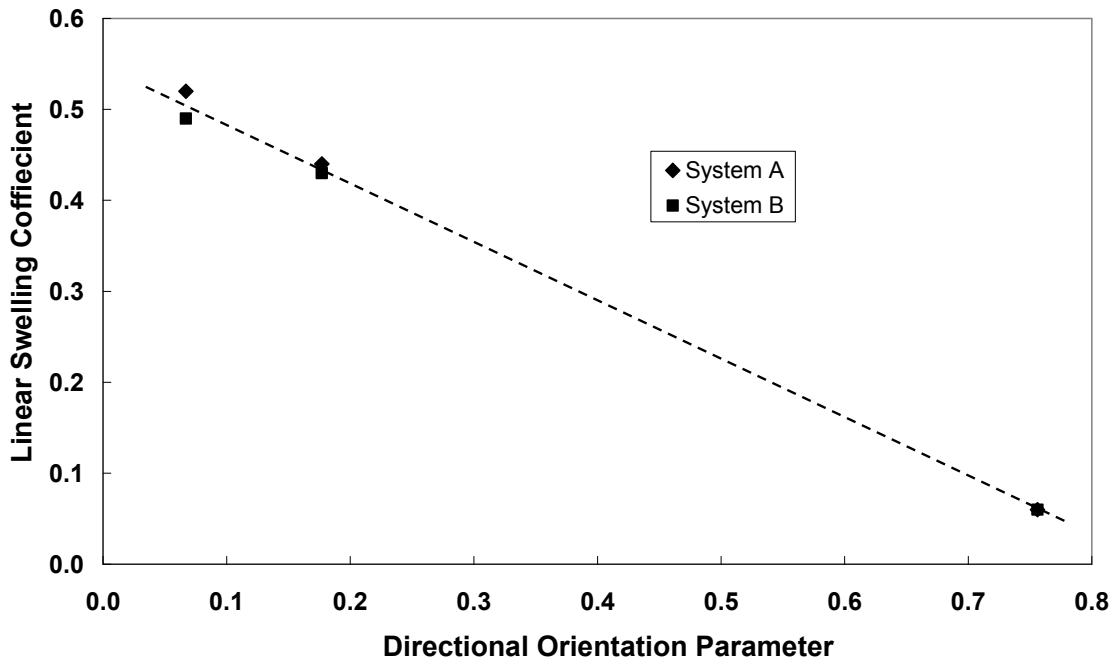


Figure 16 Relationship of composite directional swelling coefficients and the fibre orientation parameters.